Carpathian Journal of Earth and Environmental Sciences August 2025 Vol. 20, No. 2, p.427 – 440; DOI:10.26471/cjees/2025/020/344

# THE ARSENIDES, SULFARSENIDES, AND TELLURIDES ASSOCIATED WITH THE RĂZOARE Fe-Mn DEPOSIT, PRELUCA MOUNTAINS, ROMANIA

**Paulina HÎRTOPANU[1], Sorin S. UDUBAȘA[1*], Delia DUMITRAȘ[2], Daniela GHEORGHE[1]**

*[1]University of Bucharest, Faculty of Geology and Geophysics, 1, N. Bălcescu Blvd.; paulinahirtopanu@hotmail.com*
*[2]Geological Institute of Romania, 1 Caransebeș Str., Sector 1, RO-012271, Bucharest.*
*[*]Corresponding author: sorin.udubasa@gmail.com*

**Abstract:** In the Răzoare deposit the Fe:Mn ratio seems to characterize both the lower part, with Mn>Fe, and the upper part, with Mn<Fe, of the ore-bearing sequence. The lower part is dominated by an assemblage composed of tephroite, manganese humites, jacobsite, and rhodochrosite and the upper part is amphibole-dominated, typically containing clino-suenoite (formerly "manganocummingtonite"), clino-ferro-suenoite (formerly "manganogrünerite"), spessartine, magnetite, pyrrhotite, and pyrite. The middle part is dominated by manganoan fayalite, manganoan ferrosilite, and spessartine. The Răzoare tephroite - manganese humites - jacobsite assemblage has a highly restrictive mineralogical and chemical composition. The presence of Ni, Co, Sb, Mn, and Fe arsenides/antimonides and sulfarsenides/sulfantimonides is one of the striking features of this assemblage. The Ni-monoarsenides and Ni-monoantimonides, Ni-, Ni-Co, Co-, Fe and Mn diarsenides, triarsenides, and sulfarsenides were identified by light microscopy, X-ray, and SEM analyses. These minerals exhibit a wide range of isomorphic substitutions among Ni, Co, Mn, and Fe. Notably, the Mn content is higher than that of Fe, and some of these minerals contain chlorine. Their zoning reflects sudden changes in the composition of hydrothermal fluids and depict a polyphase evolution. Later minerals overgrow and replace earlier ones. The trend of mineralogical evolution was gradual, from initially Ni-Co monoarsenides with low As to higher content of As and Co (diarsenides and triarsenides) and finally, the enrichment in S allowed the deposition of the sulfoarsenides and sulfides. The Ni, Co, Mn, Fe arsenides/antimonides and sulfarsenides/sulfantimonides are genetically associated with the local hydrothermal activity that accompanied later lower-grade metamorphism. In the upper and middle parts of the deposit occur arsenides rich in Fe and sulfarsenides, bismuthinides, native Bi, and tellurides. Gold occurs associated with jacobsite in the Mn-rich assemblage, and with magnetite and pyrrhotite in Fe-rich assemblage. The mineralogical changes continued with the appearance of a large variety of manganese arsenates at the expense of arsenides.

**Keywords**: Mn-rich and Fe-rich assemblages, Ni-, Co-, Sb-, Mn-, Fe-arsenides/sulfarsenides, Bi-tellurides, sulfides, native Bi and Au, SEM analyses, low-grade metamorphic hydrothermal genesis, arsenates.

## 1. GEOLOGICAL SETTING AND MINERALOGY OF RĂZOARE Mn-Fe DEPOSIT

The Răzoare Mn-Fe deposit is located in the Preluca Mts., an "island" of Precambrian metamorphic rocks within a Tertiary sedimentary environment. It is a stratiform concentration of manganese and iron minerals, showing evidence of regional metamorphism under conditions ranging from amphibolite to granulite facies. The ore consists of silicates, carbonates, phosphates, oxides, and sulfides forming lenses of up to 60 m thick. These lenses are invariably enveloped by nearly continuous bands of black quartzite reaching a maximum thickness of about 2 m. The deposit is enclosed in a sequence of kyanite-bearing mica schists, paragneisses, amphibolites, and carbonate rocks. At least three metamorphic events have been recognized in both the host metamorphic rocks and the ores. The main six old metamorphic assemblages/types of Mn-Fe ores have been established at the Răzoare deposit: Mn-fayalite - Mn-orthopyroxene - Mn-magnetite, tephroite

- manganese humites, pyroxmangite, clino-ferro-suenoite (formerly "mangan-grünerite"/ "dannemorite", Oberti et al., 2018) – clino-suenoite (formerly "mangan–cummingtonite", Oberti et al., 2018), spessartine, and magnetite–pyrrhotite–chalcopyrite–pyrite. These assemblages displayed different positions within the ore-bearing sequence. Its bottom is defined by the rhodochrosite-rich assemblage containing jacobsite, rhodochrosite, and apatite. It is followed by an assemblage composed of tephroite, manganese humites, jacobsite, and rhodochrosite. The middle part is dominated by manganoan fayalite-manganoan ferrosilite. The upper part of the sequence is amphibole-dominated, typically containing spessartine, clino-ferro-suenoite, clino-suenoite, magnetite, pyrrhotite, and pyrite. The Fe:Mn ratio seems to characterize both the lower part with Mn>Fe, and the upper part with Fe>Mn, of the ore-bearing sequence.

The complex mineralogical composition of the ore suggests a polyphase metamorphic evolution. From the high metamorphic conditions of high amphibolites/granulite facies, the ore underwent very low metamorphic zeolite facies, under which occurred the assemblages of Ni-Co-Mn-Fe arsenides and sulfarsenides, antimonides and sulfantimonides, Bi-tellurides, sulfides, native Bi and Au. A large variety of manganese arsenates occur as oxidation products of arsenides and sulfarsenides.

The manganese-rich tephroite-manganese humites-jacobsite assemblage forms bands/lenses up to 2 m thick inside the lower rich rhodochrosite part of the ore sequences. The most striking feature of this assemblage is its restrictive chemical and mineralogical composition. The Fe content is negligible as compared to the other assemblages of the ore, practically being present only in the jacobsite composition. The tephroite associated with jacobsite and rhodochrosite is almost a pure term. Many terms of the manganese humites have been determined: sonolite, alleghanyite, ribbeite, manganhumite, leucophoenicite, and jerrygibbsite (Hîrtopanu et al., 1993). They are intimately intergrown with jacobsite and rhodochrosite and between them. Under the microscope, they are colorless and light pink. The polysynthetic twins have always been present. The arsenides and sulfarsenides of Ni-Co-Mn-Fe occur in thin veinlets and nests of a millimeter, rarely centimeter dimensions, in this Mn-rich assemblage.

The bands of iron-rich assemblage in the middle and upper parts of the deposit is dominated by the manganoan fayalite, clino-ferro-suenoite / clino-suenoite, spessartine, magnetite, pyrrhotite, and pyrite assemblage. The pyrrhotite is sometimes accompanied by chalcopyrite and pentlandite. The pyrite aggregates of large crystals were formed either by substitution of pyrrhotite or by direct deposition from hydrothermal solutions. Locally, the pyrrhotite is completely altered to a lamellar intermediary product of fine aggregates of secondary pyrite-magnetite-marcasite. Globular grains of pyrrhotite enclosed in silicates have also been observed. Some grains of pyrrhotite are oxidized and replaced by Fe-oxyhydroxides, Fe-sulfates, and secondary Fe-silicates (hisingerite). The late pyrite cemented the early manganese silicates and has small graphite and magnetite inclusions. The rare sphalerite has an iron-rich composition.

A large variation of many terms of arsenides and sulfoarsenides of Co, Ni, Mn, Fe, and the less present galenobismutite, bismuthinite, some antimonides, Bi-tellurides, native gold, and native bismuth, have been determined optically (in transmitted and reflected light), by scanning electron microscopy (SEM), and with X-ray analyses, in the Fe rich assemblages. The present paper aims to present the results of the performed laboratory work to determine these minerals.

## 2. METHODS OF INVESTIGATION

More than 40 manganese ore samples from Răzoare adits and waste dumps were collected to be analyzed. Selected samples underwent mineralogical and microtextural characterization by optical microscopy under transmitted and reflected light, and also under reflected light with oil immersion, realized mainly in the Camborne School of Mines (CSM) laboratories, University of Exeter, UK.

The best interesting samples have been also studied in the CSM laboratories by scanning electron microscopy (SEM), while represented quantitative microanalyses of arsenides and sulfoarsenides were performed by scanning microscopy with electron diffraction spectra system (SEM-EDS). The crystallochemical formulae calculations were made using the anion-based method, which reflects expected anion roles and oxidation state compatibility for the studied minerals. The BSE images were made by CAMSCAN 4DV scanning electron microscopy. The EDS method is the best for the determination of rare minerals, like ours, and is very frequently appreciated in the mineralogical literature, just the simplified one. The BSE images were made by CAMSCAN 4DV scanning electron microscope.

The XRD patterns of the representative samples were recorded using Brucker (AXS) D8 Advance diffractometer (Karlsruhe, Germany) by the Laboratory of Radiometry and X-ray, Geological Institute of Romania (Bucharest). This diffractometer used Ni-filtered CuKα radiation, a step size of 0.02° 2θ, and a counting time of 6 s per step. An operating voltage of 40 kV for a current of 30 mA, a slit system of 1/0.1/1 with a receiving slit of 0.6 mm, and a scanning range of 4 to

90° 2θ were used for measurements.

## 3. THE OPTICAL STUDY OF Ni-Co-Mn-Fe ARSENIDES/SULFARSENIDES

### 3.1. The optical study of Ni-Co-Mn-Fe arsenides/sulfarsenides of Mn-rich assemblage

Although the arsenides and sulfarsenides occur in very small/microscopic veins and nests, they have a large variation, in the same grain. The appearance of many varieties of Ni-Co-Mn-Fe arsenides/ sulfarsenides may be attributed to a small but intensely developed metamorphic hydrothermal system. A large variation of many terms of these minerals has been genetically linked with tephroite - manganese humite – jacobsite - rhodochrosite assemblage. The triarsenides, skutterudite and nickelskutterudite are the As richest among the Ni-Co-Mn-Fe arsenides. Although the Mn and Fe have low contents in the Răzoare skutterudites, the Mn content is always higher than that of Fe (Tables 1, 2, and 3). In Figure 1 (left), the white rare large nickel skutterudite grain and small white cobaltite grown secondary around the jacobsite grain can be seen. In Figure 1 (right), the large white nickelskutterudite grain occurs among the jacobsite and sonolite grains and has relics of jacobsite. In Figure 2 (left), undetermined very small yellow and white rounded/lacy arsenide/sulfarsenide grains grow around large jacobsite crystals. In Figure 2 (right), very small white and yellow rounded/lacy arsenide/ sulfarsenide grains occur around large tephroite and jacobsite crystals, and inside rhodochrosite as isolated rounded grains, or as very thin veins. The triarsenides, skutterudite and nickelskutterudite are the As richest arsenides. The group of skutterudite minerals crystallizes after diarsenides, the last one being older and deposited from hydrothermal fluids at low sulfur activity. In reflected light, the Ni, Co arsenides and sulfarsenides occur as isolate grains, among and inside the tephroite, and around the jacobsite. One can see that the Co, Ni arsenides and sulfarsenides occur more frequently with jacobsite than with manganese humites.

The arsenides and sulfarsenides were studied in reflected light in oil immersion. In Figure 3 (left), small white grains of nikelskutterudite grow around large light grey jacobsite grains, and gersdorffite occurs around jacobsite as isolated grains in the manganese humites.

In Figure 3 (right), the small rounded rammelsbergite grain grows on a large jacobsite crystal. In Figure 4 (left), the rammelsbergite (light grey, top) and gersdorffite (grey) occur together in the same small grain inside the tephroite crystals. In the same image, an irregularly shaped, unzoned grain of two phases was also observed in tephroite (Figure 4 left, right corner, bottom): half of the grain is bright yellow, anisotropic in reflected light (RL), whose SEM composition corresponds to rammelsbergite, and the other half is white, isotropic in RL, whose SEM composition corresponds to the gersdorffite. In RL in oil immersion, native gold was also determined, of micron dimension, in the cracks of the jacobsite (Figure 4 right) (Hîrtopanu and Udubaşa, 2015).

### 3.2. The optical study of Ni-Co-Mn-Fe arsenides/sulfarsenides of the Fe-rich assemblage

In the rich Fe assemblage, the manganoan fayalite - clino-suenoite - magnetite - spessartine - pyrrhotite, some Fe-rich arsenides/sulfarsenides, galenobismuthite, and native gold were determined in reflected light. The small galenobismuthite grains grow around the large pyrrhotite crystal in manganoan fayalite (Figure 6 left). In the cracks of the pyrrhotite (Figure 5 left) and magnetite (Figure 5 right) occur minute gold grains (Udubaşa and Hîrtopanu, 1995).

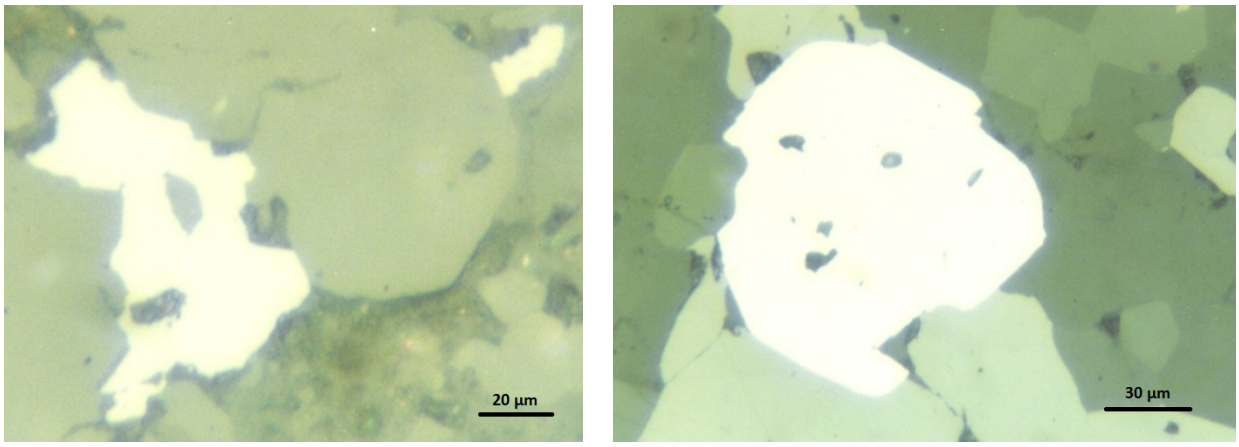


Figure 1. Nickelskutterudite (white, large) with small jacobsite relics, cobaltite (small prism, light yellow, right top corner), and jacobsite (large greenish), RL, NII, sample Rz601 (left); Nickelskutterudite (large white grain with jacobsite relics), jacobsite (light green), and sonolite (dark green), RL, NII, sample Rz80 (right).

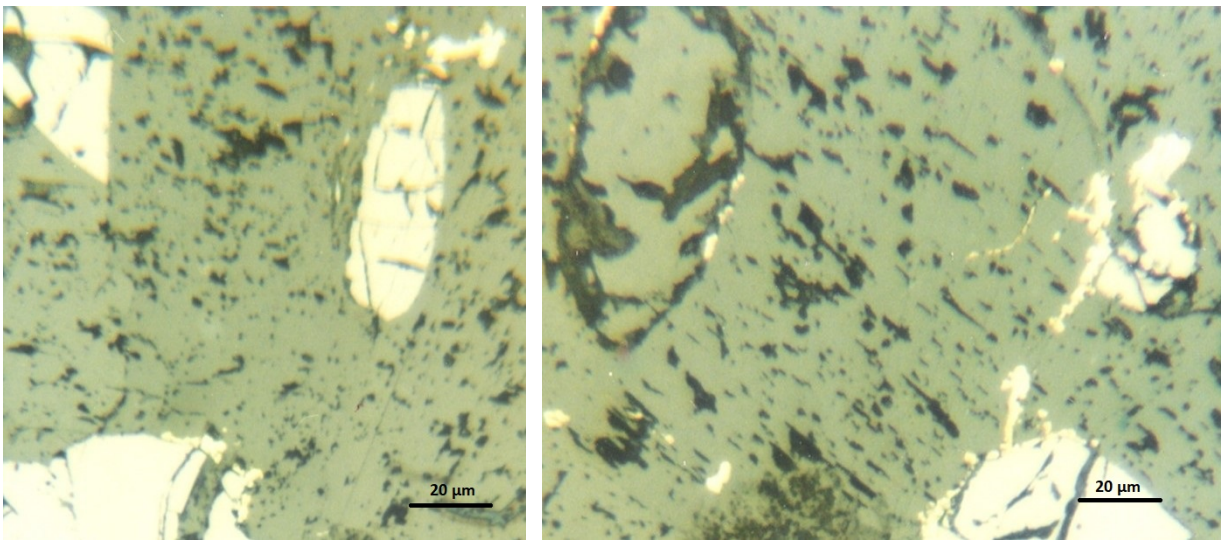


Figure 2. Arsenides/sulfarsenides (small, yellow, lacy grains near and above large white jacobsite top and left bottom) in rhodochrosite (green) (left); Arsenides/sulfarsenides (very small, yellow, white, lacy, rounded grains around large tephroite (top left) and jacobsite (right corner), and isolate small grains in rhodochrosite (right); RL, NII.

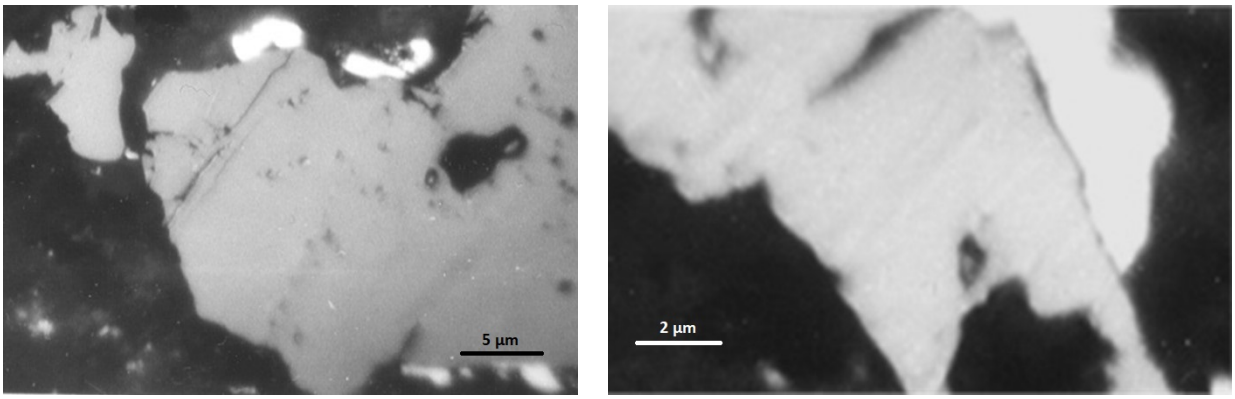


Figure 3. Jacobsite grain (large, grey) with nickelskutterudite (two, small, white, rounded, upper part), gersdorffite (white grey, top left corner, and small grains, bottom right corner), RL, NII, oil immersion (left); Jacobsite (large, light grey), rammelsbergite (white, top right), RL, NII, oil immersion (right).

## 4. SEM ANALYSES OF Ni, Co, Mn, Fe ARSENIDES/SULFARSENIDES

### 4.1. SEM analyses of Ni, Co, Mn, Fe arsenides/sulfarsenides of the Mn-rich assemblage

The optical study of the Răzoare arsenides/sulfarsenides was partially completed by scanning electron microscopy (SEM) analyses. The results are illustrated by the electron diffractogram spectra, backscattered electron images, and a few representative compositional chemical analyses.

In the backscattered image of Figure 6 left the gersdorffite (NiAsS), which is a sulfarsenide, grows zoned around rammelsbergite ($NiAs_2$), which is a diarsenide. These textural relations show that the diarsenides are older than sulfarsenides, and the As content decreases from the diarsenides to the sulfarsenides. In the backscattered electron image of Figure 6 right an irregularly zoned grain of sample Rz527 has a high compositional variation, which can be seen in Table 1.

The maucherite (points 1-3) occurs as rounded relics in a mixture of rammelsbergite and cobaltian gersdorffite. The maucherite seems to be the oldest monoarsenide of the zoned grain and manganoan gersdorffite (Point 7) is the latest.

The crystallochemical formulae of these minerals of the same zoned grain, are the following:
Point 1: $(Ni_{11,89}Co_{0,06}Mn_{0,06}Fe_{0,01})As_{6,86}S_{0,07}Cl_{0,04}$ Maucherite,
Point 2: $(Ni_{11,52}Mn_{0,29}Fe_{0,07})As_{6,05}S_{0,15}Cl_{0,93}$ Maucherite,
Point 3: $(Ni_{11,45}Mn_{0,28}Fe_{0,05})As_{6,40}S_{0,16}Cl_{0,67}$ Maucherite,
Point 4: $(Ni_{1,23}Co_{0,04}Mn_{0,03}Fe_{0,02})As_{0,79}S_{1,21}$ Gersdorffite,
Point 5: $(Ni_{0,91}Co_{0,32}Mn_{0,09}Fe_{0,14})As_{1,04}S_{0,96}$ Gersdorffite-cobaltite ss.,
Point 6: $(Ni_{1,42}Co_{0,02}Mn_{0,04}Fe_{0,03})As_{1,12}S_{0,88}$ Gersdorffite,
Point 7: $(Ni_{1,23}Co_{0,01}Mn_{0,12}Fe_{0,05})As_{0,75}S_{1,25}$

Gersdorffite manganoan.

The simplified formula of the above 1-7 points are: 1. NiAs; 2. Ni(As, Cl); 3. Ni(As, Cl); 4. Ni(S, As); 5. (Ni, Co, Fe, Mn)(As, S); 6. Ni(As, S); 7. (Ni, Mn)(S, As).

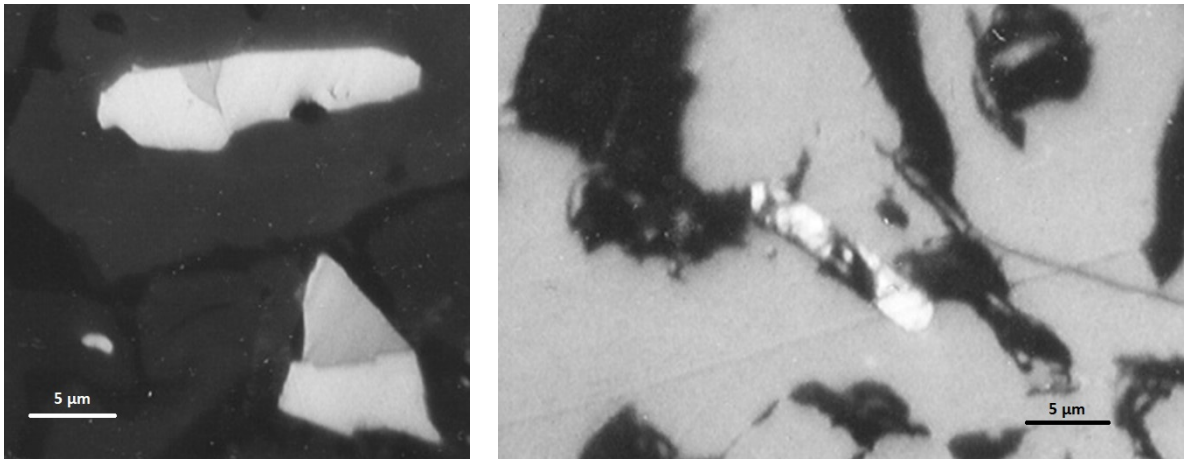


Figure 4. Rammelsbergite (light grey) and gersdorffite (grey) inside tephroite (dark grey) (left); Gold (small bright white prism) grown on the cracks of jacobsite (large, white grey) (right); RL, NII, oil immersion.

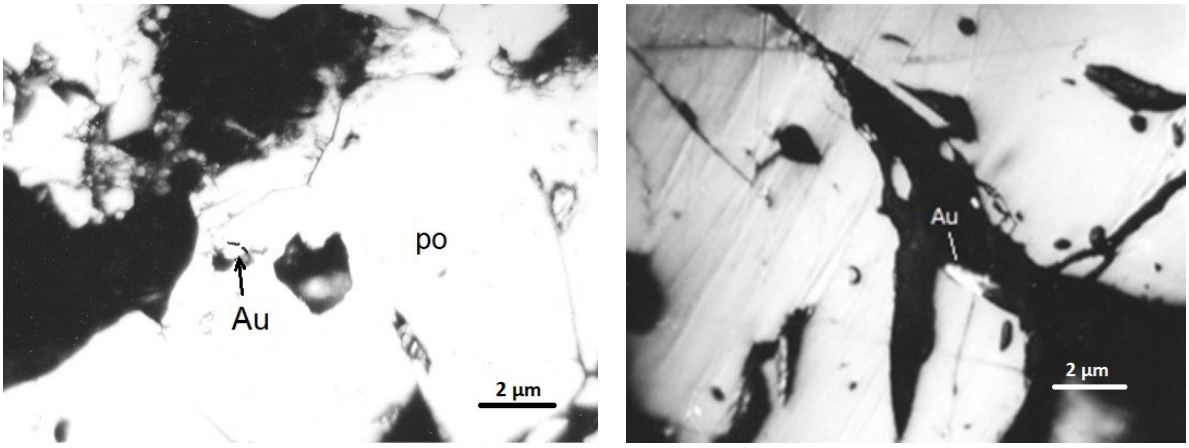


Figure 5. Pyrrhotite (po, large), galenobismuthite (small, white, left and top, around pyrrhotite), gold (Au, white bright) (left); Gold (small bright white) on the crack of magnetite (large, white); RL, NII, oil immersion.

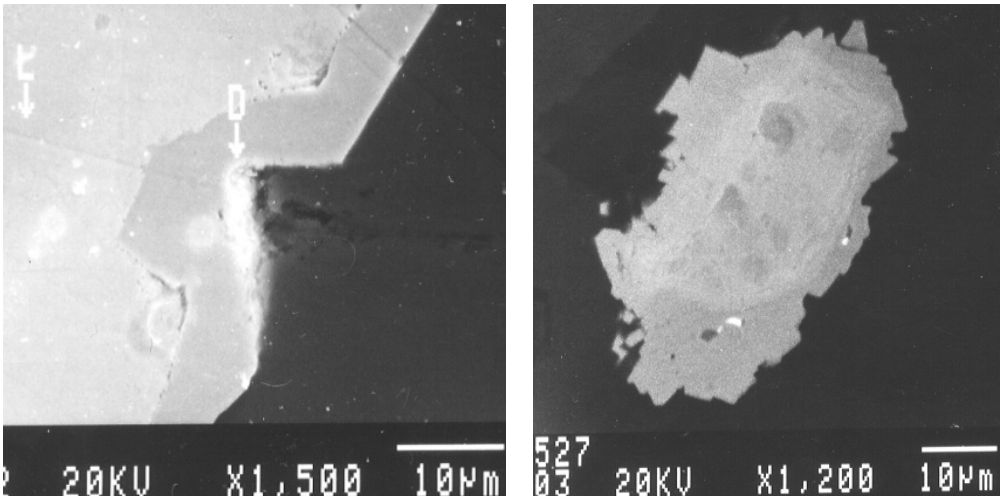


Figure 6. Backscattered electron image of zoned grain: rammelsbergite (L, light grey, left), gersdorffite (D, grey, rim) in sonolite (dark grey) (left); Backscattered electron image of irregularly zoned grain: maucherite with Cl (small rounded dark grey, centre, isolated nodules points 1-3) relics in two mixed phases: gersdorffite (white grey, point 4) and cobaltian gersdorffite (white, point 5), and on the rim gersdorffite (white grey, up and left, pct. 6) + manganoan gersdorffite (grey, bottom and right, point 7) (right); See their compositional variation in Table 1, sample Rz527.

Table 1. The variation of the representative composition of arsenides/sulfarsenides of zoned grain in sample Rz527, from the core (point 1) to the rim (point 7) (Analyst: Antony Ball).

| Point 1 | | Point 2 | | Point 3 centre | | Point 4 dark phase | | Point 5 light phase | | Point 6 | | Point 7 | |
|---|---|---|---|---|---|---|---|---|---|---|---|---|---|
| Elem. | Atom% | Elem. | Atom% | Elem. | Atom% | Elem. | Atom% | Elem. | Atom% | Elem. | Atom% | Elem. | Atom% |
| Ni | 62.590 | Ni | 60.651 | Ni | 60.256 | Ni | 37.000 | Ni | 26.339 | Ni | 40.396 | Ni | 36.235 |
| As | 36.101 | As | 31.851 | As | 33.666 | As | 23.795 | As | 30.151 | As | 31.956 | As | 21.888 |
| Fe | 0.076 | Fe | 0.352 | Fe | 0.275 | Fe | 0. 629 | Fe | 3.935 | Fe | 0.737 | Fe | 1.365 |
| Co | 0.307 | Co | n.d. | Co | n.d. | Co | 1.296 | Co | 9.317 | Co | 0.686 | Co | 0.161 |
| Mn | 0.339 | Mn | 1.505 | Mn | 1.471 | Mn | 0.762 | Mn | 2.685 | Mn | 1.167 | Mn | 3.529 |
| S | 0.385 | S | 0.768 | S | 0.824 | S | 36.518 | S | 27.573 | S | 25.058 | S | 36.822 |
| Cl | 0.202 | Cl | 4.873 | Cl | 3.508 | Cl | n.d. | Cl | n.d. | Cl | n.d. | Cl | n.d. |

Points 1, 2, and 3 of Table 1 have a maucherite composition with high Ni, less As, a few Mn which substitutes Ni, and relatively high Cl content. In the backscattered image of Figure 6 (right), these compositions correspond to the dark relics rounded grey grains in the core of the zoned grain. Points 4 and 5 correspond to the central area where the maucherite relics are enclosed. There are two mixed phases: point 4 dark grey on the image, corresponds to gersdorffite composition, and point 5, the light grey phase, corresponds to a gersdorffite-cobaltite solid solutions composition, and both do not have Cl. The rim of the last band of the grain has a gersdorffite composition (Point 6), which changes in the same band in Point 7, with high S and less As, Ni, and Co, and relatively high Mn and low Fe contents, corresponding to the gersdorffite / gersdorffite-cobaltite solid solution. In the backscattered image of Figure 6 (right) the rim band is grey with different shades: dark grey in the bottom, the right, and upper part of the rim corresponding to gersdorffite, and light grey on the left part of the rim band is gersdorffite-cobaltite solid solution, reflecting the chemical variation in the same band of zoned grain.

In the other zoned grains of the same sample, the maucherite and gersdorfitte with chlorine contents (3-5 wt.%) have the following zonation: Ni, As, Cl in the center, Ni, As, S, Cl on the rims, and Ni, As, S with no Cl between them, in the middle of the grain. Other grains have Ni, As, and Cl in the center and Ni, As, S, and Cl marginally. Many zoned grains have Ni arsenides with Cl in the center and sulfarsenides without Cl on the rims. The mineralizing process was multistage with sudden fluctuations in the composition of the hydrothermal fluids.

The variation of representative compositions of the arsenides/sulfarsenides of the other zoned grain of the same sample (Rz527), from core to rim is presented in Table 2. Point 1 with high Ni and As composition, low Co, and higher Mn than Fe, corresponds most probably to manganoan maucherite, which is a monoarsenide. The Ni is substituted by Mn with a relatively high value (9.446 wt.%), so it could be considered a manganoan variety. The Co has low content, and Fe and S have very low content. Points 2, 3, 4, and 5 have a maucherite composition, with high Ni and less As, and low variable values of Co and Mn. There is a wide range of isomorphic substitutions among Ni, Co, As, Mn, and Fe inside Ni-Co-As-Mn-Fe arsenides. The compositions of points 6 and 7, with less As and high S, belong to manganoan gersdorffite mixed with some cobaltite solid solution.

The crystallochemical formulae of the mineral compositions of the same zoned grain of the sample Rz527 from Table 2, are the following:

Point 1: $(Ni_{10,55}Co_{0,62}Mn_{0,90}Fe_{0,07})As_{6,83}S_{0,02,}$ Maucherite, manganoan,

Point 2: $(Ni_{9,71}Co_{1,87}Mn_{0,31})As_{7,07}S_{0,03}$, Maucherite, cobaltian,

Point 3: $(Ni_{9,95}Co_{1,35}Mn_{0,86}Fe_{0,09})As_{6,72}S_{0,03}$, Maucherite, cobaltian, manganoan,

Point 4: $(Ni_{9,89}Co_{1,66}Mn_{0,46}Fe_{0,04})As_{6,94}S_{0,01}$, Maucherite, cobaltian,

Point 5: $(Ni_{9,57}Co_{1,57}Mn_{1,03}Fe_{0,06})As_{7,76}S_{0,21}$, Maucherite, manganoan,

Point 6: $(Ni_{1,02}Co_{0,32}Mn_{0,23}Fe_{0,01})As_{0,78}S_{1,22}$, Gersdorffite, cobaltian manganoan,

Table 2. The variation of the representative composition of arsenides/sulfarsenides of zoned grain in sample Rz527, from core (point 1) to rim (point 7) (Analyst: Antony Ball).

| Point 1 | | Point 2 | | Point 3 | | Point 4 | | Point 5 | | Point 6 | | Point 7 | |
|---|---|---|---|---|---|---|---|---|---|---|---|---|---|
| Elem. | Atom% | Elem. | Atom% | Elem. | Atom% | Elem. | Atom% | Elem. | Atom% | Elem. | Atom% | Elem. | Atom% |
| As | 35.958 | As | 37.235 | As | 35.392 | As | 36.515 | As | 34.481 | As | 21.904 | As | 20.459 |
| Co | 3.270 | Co | 9.860 | Co | 7.094 | Co | 8.731 | Co | 8.286 | Co | 8.922 | Co | 4.426 |
| Ni | 55.549 | Ni | 51.121 | Ni | 52.384 | Ni | 52.040 | Ni | 50.382 | Ni | 28.445 | Ni | 29.032 |
| S | 0.122 | S | 0.168 | S | 0.145 | S | 0.075 | S | 1.085 | S | 33.979 | S | 36.175 |
| Mn | 4.752 | Mn | 1.616 | Mn | 4.515 | Mn | 2.438 | Mn | 5.445 | Mn | 6.427 | Mn | 9.446 |
| Fe | 0.349 | Fe | n.d. | Fe | 0.470 | Fe | 0.201 | Fe | 0.321 | Fe | 0.323 | Fe | 0.462 |

Table 3. The variation of the representative composition of arsenides/sulfarsenides of zoned grain in sample Rz601 (Analyst: Antony Ball).

| Point 1 | | Point 2 | | Point 3 | | Point 4 | | Point 5 | |
|---|---|---|---|---|---|---|---|---|---|
| Elem. | Atom% | Elem. | Atom% | Elem. | Atom% | Elem. | Atom% | Elem. | Atom% |
| Ni | 54.117 | Ni | 48.667 | Ni | 1.563 | Ni | 58.915 | Ni | 11.577 |
| Co | 6.042 | Co | 10.780 | Co | 30.790 | Co | 0.582 | Co | 18.230 |
| As | 36.043 | As | 36.677 | As | 20.042 | As | 35.613 | As | 20.146 |
| S | 0.290 | S | 0.292 | S | 42.930 | S | 0.105 | S | 42.653 |
| Mn | 2.814 | Mn | 3.066 | Mn | 4.394 | Mn | 4.732 | Mn | 4.201 |
| Fe | 0.694 | Fe | 0.518 | Fe | 0.281 | Fe | 0.053 | Fe | 3.193 |

Point 7: $(Ni_{1,03}Co_{0,16}Mn_{0,33}Fe_{0,02})As_{0,72}S_{1,28}$, Gersdorffite, cobaltian manganoan.

The simplified chemical formulae of these mineral compositions, corresponding to the above 1-7 points are: 1. (Ni, Mn)As; 2. (Ni, Co)As; 3. (Ni, Co, Mn)As; 4.(Ni, Co)As; 5. (Ni, Co, Mn)As; 6. (Ni, Co, Mn)(As, S); 7. (Ni, Mn, Co)$AsS_2$.

The compositional variation of other arsenides/sulfarsenides in the same zoned grain, from core to rim of sample Rz601, can be seen in Table 3.

In Table 3, points 1 and 2, in the core of grain, with high Ni and less As, Mn higher than Fe, and relatively high Co contents, correspond to maucherite/cobaltian maucherite. The composition of point 3, which is zoned on the composition of point 2, has high Co, and S, and low Ni and Fe content, which could correspond to the solid solution cobaltite-gersdorffite series. It is a manganoan variety. The composition of point 4, zoned on that of point 3, situated in the middle of the zoned grain, has a sudden modification of its composition and shows again a maucherite composition, which could be considered a second maucherite generation, the first one being in the core of the grain (point 1). The composition of point 5, which is zoned on the composition of point 4, has also a sudden modification, and has average values of Ni and Co, higher S than As, corresponding to manganoan Ni-rich cobaltite-gersdorffite solid solution series, forming the rim of the zoned grain.

The crystallochemical formulae of these minerals of zoned grain in Table 3, sample Rz601, are:

Point 1: $(Ni_{11,92}Co_{1,33}Mn_{0,62}Fe_{0,15})As_{7,94}S_{0,06}$, cobaltian maucherite solid solution series,

Point 2: $(Ni_{10,53}Co_{2,33}Mn_{0,66}Fe_{0,11})As_{7,94}S_{0,06}$, manganoan cobaltian maucherite solid solution series,

Point 3: $(Co_{0,98}Ni_{0,05}Mn_{0,14}Fe_{0,01})As_{0,64}S_{1,36}$, manganoan cobaltite-gersdorffite solid solution series,

Point 4: $(Ni_{13,20}Co_{0,13}Mn_{1,06}Fe_{0,01})As_{7,98}S_{0,02}$, manganoan maucherite,

Point 5: $(Co_{0,58}Ni_{0,37}Mn_{0,13}Fe_{0,10})As_{0,64}S_{1,36}$, manganoan cobaltite-gersdorffite solid solution series.

The simplified chemical formulae corresponding to above points 1-5 could be written as: 1. (Ni, Co)As; 2. (Ni, Co, Mn)As; 3. (Co, Mn)$AsS_2$; 4. (Ni, Mn)As; 5. (Co, Ni, Mn, Fe)$AsS_2$.

In the sample Rz527 some zoned grains have the niccolite composition in the core and modderite on the rims, both chemical compositions being appreciated by SEM analyses. Frequently, many zoned grains have Ni arsenides in the cores and sulfarsenides on the edges. The mineralizing process was multistage with sudden fluctuations of the composition of the mineralizing fluids. In this polished thin section were also observed other arsenide/sulfarsenide grains with zoned textures. A zoned grain with 3 phases in reflected light: orange and anisotropic in the core which has a maucherite composition, white isotropic in the middle in RL, which has a linnaeite composition, and bluish isotropic in reflected light, on the rim of the grain, with a gersdorffite composition. Other grains with zoned texture: (a) orange and anisotropic in RL has in the core a nickeline composition (b) yellow and isotropic in RL, in the middle has a cobalt-gersdorffite composition, and (c) bluish and isotropic in RL, on the rim, has a gersdorffite composition.

In the polished thin section Rz601, some millimetric isometric grains with rounded/irregular rims have a yellow-reddish color and present alterations on their surfaces in RL. They have high Ni and lower As compositions, no Co, Fe, and S. Their SEM composition corresponds to maucherite. Near maucherite a long prism grain has a white-bluish color in RL, and a composition with higher As, which could correspond to rammelsbergite. In the same polished thin section, a prismatic/acicular grain has zoned texture in RL: the core is orange, whose composition shows on SEM analyses As, Ni, Co corresponding to nickelskutterudite, and the rim is yellowish green, whose As, Ni, Co, and S composition corresponds to that of the cobaltian gersdorffite. On a thin vein of the same PTS were observed in RL 3 lacy small anisotropic grains with high reflectivity, whose compositions of CoAsS correspond to that of cobaltites. Near them, a small acicular yellow grain in RL has at SEM an As, Ni, and Co composition, which corresponds to cobaltian rammelsbergite. On the jacobsite fine cracks, in the same sample occur many isotropic prismatic white grains with NiAsCo composition, whose SEM values correspond to that of the nickelskutterudites.

The Răzoare arsenides/sulfarsenides have large compositional variations: gersdorffite has sometimes high As content and rammelsbergite high Ni content. The maucherite sometimes has Cl content. The gersdorffite forms a solid solution series with cobaltite, and the rammelsbergite forms a continuous solid solution series with löellingite and safflorite (Spiridonov and Gritsenko, 2007). Generally, the monoarsenides, diarsenides and triarsenides occur as zoned grains and are surrounded by sulfarsenides. During each generation, Ni-Co diarsenides were deposited earlier than the Ni-Co-Mn-Fe triarsenides. The nickelskutterudite, a triarsenide, forms two compositional series: skutterudite - nickelskutterudite and skutterudite - manganskutterudite. Nickelskutterudite is earlier than skutterudite and manganskutterudite. The Co-Ni-Mn-Fe triarsenides, skutterudite, nickelskutterudite, manganskutterudite, form continuous isomorphic series (Spiridonov and Gritsenko, 2007). The skutterudite group crystallizes at low sulphur activity and it is the As richest arsenide of Ni-Co-Mn (Spiridonov and Gritsenko, 2007).

### 4.2. SEM analyses of Ni, Co, Mn, Fe arsenides, sulfarsenides, and Bi-tellurides of the Fe-rich assemblage

The iron-rich arsenides and sulfarsenides are genetically linked with the pyrrhotite – chalcopyrite - pyrite association, which belong to Fe-rich Mn-fayalite - Mn-ferrosilite - clino-suenoite - clino-ferro-suenoite - spessartine - magnetite assemblage. The löllingite and arsenopyrite occur relatively frequently, while the other arsenides / antimonides / sulfarsenides / sulfantimonides rarely occur, their presence being detected only by SEM and X-ray analyses performed on the ore (Table 4).

In the backscattered electron image of Figure 7, the arsenopyrite and löllingite are associated with manganoan fayalite. The löllingite (3), which is a diarsenide, has high As, high Fe, and very low Ni, Mn, and S. The arsenopyrite (2), which is a sulfarsenide, has high S, less As and Fe, and very low Mn and Ni. There is a good correlation among the compositions of coexisting manganoan fayalite and these arsenides/sulfarsenides, as it happens in the tephroite/manganese humites/jacobsite/rhodochrosite assemblage. The textural relations between them show that the löllingite, ($FeAs_2$), which is a diarsenide, is older than arsenopyrite, (FeAsS), which is a sulfoarsenide, and the pyrrhotite is the oldest among them.

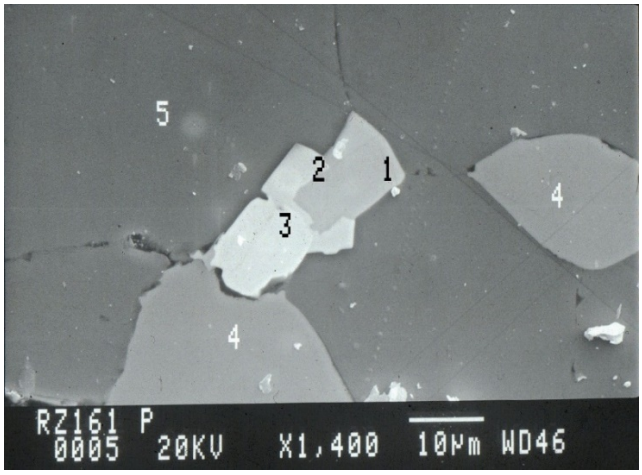

Figure 7. Backscattered electron image of pyrrhotite (1, grey), arsenopyrite (2, small white grey around pyrrhotite), löllingite (3, white), and magnetite (4, grey) in manganoan fayalite (dark grey).

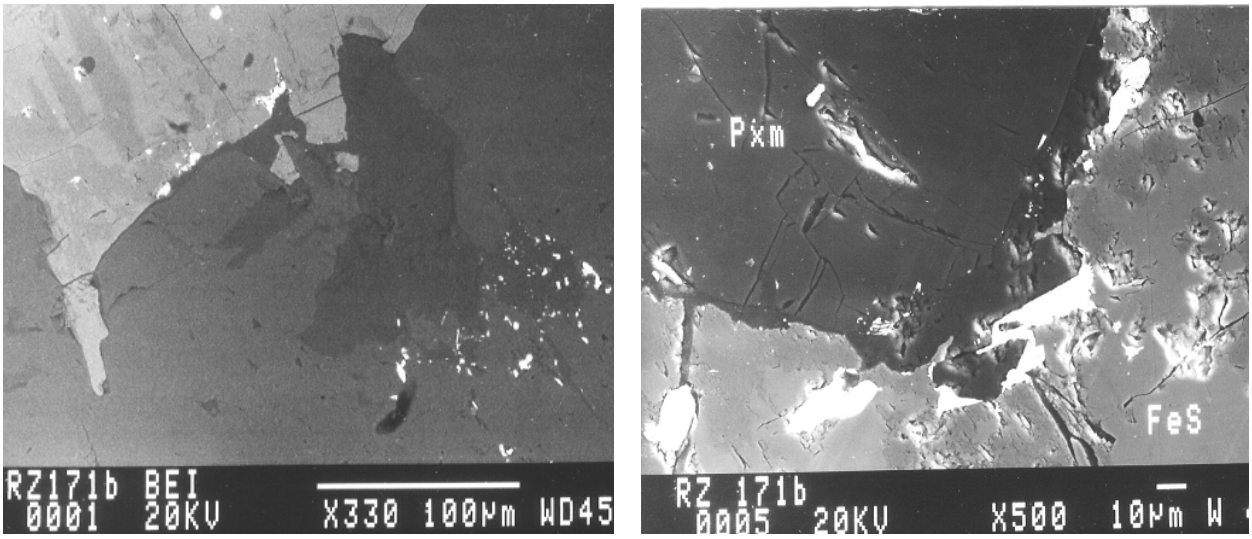

Figure 8. Backscattered electron image of vihorlatite (?) (white, small) on the cracks of garnet (dark grey) and pyrrhotite (light grey, twinned) (left); backscattered electron image of hedleyite (white bright) grown inside clino-suenoite (Pxm) and pyrrhotite (FeS) (right).

Table 4. The arsenides/sulfarsenides/antimonides/Bi-tellurides/sulfides identified in different samples in the Răzoare Mn-Fe deposit.

| Mineral | Formula | Crystal system | Sample no. |
|---|---|---|---|
| Arsenopyrite | FeAsS | monoclinic | Rz171P |
| Colusite | $Cu_3AsS_4$ | cubic | Rz132 |
| Benavidesite | $Pb_4MnSb_6S_{14}$ | monoclinic /forms a series with jamesonite | Rz606 |
| Berthierite | $FeSb_2S_4$ | monoclinic | Rz531, RzA |
| Bismuthinite | $Bi_2S_3$ | orthorhombic | 161a |
| Breithauptite | NiSb | hexagonal | Rz603, Rz504 |
| Cattierite | $CoS_2$ | cubic | Rz601 |
| Clerite | $MnSb_2S_4$ | orthorhombic | Rz79B, Rz604 |
| Cobaltite | CoAsS | orthorhombic | Rz601 |
| Füloppite | $Pb_3Sb_8S_{15}$, rich in Sb | monoclinic | Rz202, Rz105, Rz528c |
| Hedleyite | $Bi_7Te_3$ | trigonal | 171b |
| Hutchinsonite | $TlPbAs_5S_9$ | orthorhombic | Rz132 |
| Gersdorffite | NiAsS | cubic | 531d, Rz60, Rz527, Rz161 |
| Gersdorffite cobaltian | (Ni, Co)AsS | cubic | Rz601 |
| Glaucodot | (Co, Mn, Fe)AsS | orthorhombic | Rz601 |
| Kieftite | $CoSb_3$ | cubic | Rz528A, Rz79B, Rz504A, Rz504C, Rz606 |
| Lautite | CuAsS | orthorhombic | Rz60A |
| Lindströmite | $Cu_3Pb_3Bi_7S_{15}$ | orthorhombic | Rz531E, Rz528c |
| Linnaeite | $Co_2S_4$ | cubic | Rz601 |
| Löllingite | $FeAs_2$, with low Ni content | orthorhombic | Rz604, Rz161 |
| Löllingite, cobaltian | $(Fe, Co)As_2$ | orthorhombic | Rz604z |
| Modderite | (Co, Mn, Fe)As | orthorhombic | RzC, Rz601 |
| Mohite | $Cu_2SnS_3$ | triclinic | Rz525, Rz528c, Rz528A |
| Nickeline/Niccolite | NiAs | hexagonal | Rz601, Rz527 |
| Nickelskutterudite | $(Ni, Co)As_3$ | cubic | Rz80 |
| Pentlandite | $(Ni,Fe)_9S_8$ | cubic | Rz80A |
| Rammelsbergite | $NiAs_2$ | orthorhombic | Rz527, Rz601 |
| Rammelsbergite, cobaltian | $(Ni,Co)As_2$ | orthorhombic | Rz527, Rz601 |
| Safflorite | $CoAs_2$ | orthorhombic | Rz601 |
| Safflorite, ferroan | $(Co, Ni, Fe)As_2$ | orthorhombic | Rz60 |
| Skutterudite | $CoAs_3$ | cubic | Rz60, Rz504, Rz601 |
| Stibnite | $Sb_2S_3$ | orthorhombic | RzA |
| Ullmannite | NiSbS | cubic | RzA |
| Willyamite | (Co, Ni)SbS | cubic | Rz504B |

It is a characteristic of the Fe-rich assemblage in the presence of bismuthides, Bi-tellurides, Bi-sulfotellurides, Bi-sulfides (Table 4), native Bi, and native Au. The SEM study showed rare inclusions of bismuth tellurides up to the micron scale. They belong to the tetradymite group. The bismuth tellurides have a large compositional variation, with a wide range of anion substitutions. Generally, their Te content is low and the content of Bi is high. Also, the S and Se content of these tellurides are very low. In the Fe-rich assemblage occur two bismuth tellurides with no S, tellurobismuthite ($Bi_2Te_3$) and hedleyite ($Bi_7Te_3$), which also belong to the tetradymite group. In the backscattered electron image of Figure 8 (left), the low Se bismuth telluride grows on the cracks of the pyrrhotite, garnet, and on the border between them. It has high Bi, low Te, low Se, and very low Mn. This composition corresponds to the hedleyite with low Se or to vihorlatite**,** $Bi_{24}Se_{17}Te_4$, the other member of the tetradymite group with low Te and without S. The hedleyite occurs as small foliated grains on the cracks of the pyrrhotite and clino-suenoite and on the border between them (Figure 8 right). The hedleyite, a bismuth telluride without S, has high Bi, low Te, and very low Fe contents.

The native bismuth, Bi, occurs in manganoan fayalite / clino-ferro-suenoite / spessartine / pyrrhotite assemblages in close association with Bi-tellurides, especially with the tellurobismuthite. In the electron backscatterd image of Figure 9 (left) the small native Bi grains occur in the cracks of the manganoan fayalite, and on the border between manganoan fayalite and spessartine.

In the same sample, Rz171b, occurs the tellurobismuthite ($Bi_2Te_3$), a tellurobismuthite with high Te content. Its backscattered electron image in Figure 9 (right) shows the relatively large rare euhedral tellurobismuthite crystal grown on the border between pyrrhotite (FeS) and spessartine (Gr).

Benavidesite**,** $MnPb_4Sb_6S_{14}$, forms a series with jamesonite $FePb_4Sb_6S_{14}$. Benavidesite was first discovered in 1982 in the Uchucchacua mine, Peru,

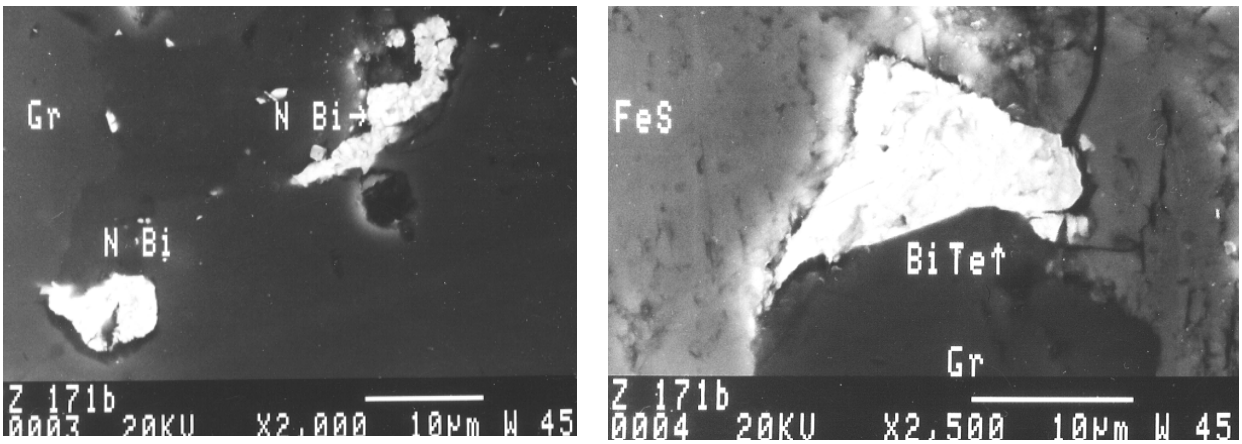


Figure 9. Backscattered electron image of native bismuth (NBi, bright white) inside manganoan fayalite (dark grey) and on the border manganoan fayalite/spessartine (Gr, dark grey) (left); Backscattered electron image of tellurobismuthite of BiTe (bright white) at the border pyrrhotite (FeS, light grey)/spessartine (Gr, dark grey).

and simultaneously in Sweden, Sätra Mine (Oudin et al., 1990). Benavidesite and jamesonite form a complete series of solid solutions, the compositions of this solid-solution series ranging from Fe-rich to Mn-rich in which jamesonite is the most abundant sulfosalt mineral. The Răzoare jamesonite forms acicular crystals in cavities, representing products of late stage processes.

X-ray Powder Pattern of Răzoare benavidesite: d spacing (Å) and Intensity ($I/I_o$): 8.20490(20); 5.07704(10); 4.10226(30); 3.88213(45); 3.44536(100); 3.15213(45); 2.82033(40); 2.84206(5); 2.74546(30); sample Rz606. They are very similar to those of Sweden benavidesite. Răzoare benavidesite occurs as microveins with thometzekite, $Pb(Cu,Zn)_2(AsO_4)_2 \cdot 2H_2O$ and quenselite $PbMn_2(OH)$, which cut the leucophoenicite-sonolite-humite association.

Hutchinsonite, $(Pb,Tl)As_5S_9$, is a very rare sulfosalt mineral of thallium, arsenic, and lead. It was first discovered in a sample from Binnenthal, Switzerland (Solly, 1905). Also, hutchinsonite occurs in the Quiruvilca mine, Peru (Nelen and White, 1985). Hutchinsonite from the Răzoare deposit occurs closely associated with ardennite, zwieselite (which forms a series with triplite), arsenoclasite, dravite, and yoshimuraite, in the Rz132 sample. These associated minerals were identified by SEM-EDS and/or XRD and described in detail in Hîrtopanu (2019).

X-ray Powder Pattern of Răzoare hutchinsonite: d spacing (Å) and Intensity ($I/I_o$): 5.34313(50); 2.74030 (100); 2.69920(80); 3.70032 (80), 4.37799(60); 4.48195 (50); 2.2233(30), 184913(30). The data are very similar to those samples of Peru hutchinsonite.

Füloppite**,** $Pb_3Sb_8S_{15}$, occurs as microveins with stibnite and benavidesite in leucophoenicite, humite, axinite-(Mg), hungchaoite, $(MgB_4O_5(OH)_4 \cdot 7H_2O)$, chlorapatite, hollandite, calcite association (minerals identified by SEM-EDS and/or XRD, for details see Hîrtopanu, 2019). X-ray powder pattern of Răzoare füloppite: d spacing (Å) and Intensity ($I/I_o$): 3.88972(100); 4.05955(20); 3.68532(50); 3.38497(70); 3.20599(90); 3.13581(50); 2.92177(80); sample Rz202.

Kieftite, $CoSb_3$, Sb analog of skutterudite, $CoAs_3$, is a new mineral species from the Tunaberg Cu-Co-sulfide skarn ores, southeastern Bergslagen, Sweden. It occurs as small tin-white subhedral to euhedral crystals in chalcopyrite, associated with bornite, galena, native bismuth, native silver, dyscrasite, gudmundite, and tetrahedrite (Dobbe et al, 1994). The Tunaberg kieftite shows Co substitution by Ni, Fe, and Cu, whereas Sb shows substitution by Cl. The Răzoare kieftite is associated with löllingite cobaltian, willyamite, jerrygibbsite, caryinite, ardennite, flinkite, bobdownsite, samfowlerite (very rare new mineral) $Ca_{14}Mn_3Zn_2Be_2Be_6Si_{14}O_{52}(OH)_6$, (Rouse et al., 1994), qandilite, karelianite, ashoverite, manganite, cadmian calcite, manganostibite, melanostibite, karelianite ($V_2O_3$), macaulayite, in Rz504 sample. In Rz79B sample the kieftite is associated with jamesonite, breithauptite, willyamite, triphylite, hopeite, kryzhanovskite, eudydimite, schoonerite, greifensteinite, and waterhouseite. All these associated minerals were identified by SEM-EDS and/or XRD, for details see Hîrtopanu (2019).

X-ray Powder Pattern of Răzoare kieftite (Rz79 sample): d spacing (Å) and Intensity ($I/I_o$): 2.85262(100); 642403(10); 3.68888(15); 2.41754(60); 2.12921(20); 1.77277(60); The data are similar with the X-ray data of Tunaberg kieftite. In the sample Rz528 the kieftite is associated with mohite ($Cu_2SnS_3$) and willyamite (Co,Ni)SbS which are microveins in rhodochrosite, hydroxylapatite, fluorapatite, hummerite, eudydimite assemblage (minerals identified by SEM-EDS and/or XRD, for details see Hîrtopanu, 2019).

Ullmanite**,** NiSbS, and Willyamite**,** (Co,Ni)SbS, were determined by X-ray analyses in sample Rz504B,

associated to secondary minerals as ilvaite (?), brucite, quandilite, macaulayite, dolomite, and karelianite (for details about the identification by SEM-EDS and/or XRD, see Hîrtopanu, 2019).

Clerite, $MnSb_2S_4$, is a new mineral approved by IMA in 1996 (Murzin et al., 1996). It was discovered in the Vorontsovskoye gold deposit, Urals Mts. The Urals clerite is associated with realgar, alabandite, sphalerite, aktashite, and routhierite (minerals identified by SEM-EDS and/or XRD, for details see Hîrtopanu, 2019). Clerite is isostructural with berthierite ($FeSb_2S_4$), being its Mn-bearing analog.

X-ray Powder Pattern of Răzoare clerite: d spacing (Å) and Intensity $I/I_o$ :7.1529(40); 4.43598(50); 3.70699(90); 3.42295(40); 2.90406(95); 2.64983(100); 2.06675(30); 1.91235(45); sample Rz604. It is very similar to the Urals clerite. The clerite from Răzoare is associated with löllingite cobaltian, djurleite, willyamite, melanostibite, manganostibite, manganite, ashoverite, fritzscheite, $Mn(UO_2)_2(PO_4,VO_4)_2 \cdot 4H_2O$), and the low hydrothermal berthierite, $FeSbS_2$, stibnite, and arsenopyrite association, which occur in the areas deficient in the sulfur of the same sample. These associated minerals were identified by SEM-EDS and/or XRD, for details see Hîrtopanu (2019).

Lindströmite, $Cu_3Pb_3Bi_7S_{15}$, occurs associated to secondary microveins which cut the primary tephroite bearing manganese humite association. The association of the microveins: gersdorffite, djurleite, stibnite, rhodochrosite, greifensteinite, chlorapatite-vanadat, vayrynenite, rossite (calcium vanadate), cadmian calcite, natrozippeite, qandilite, birnessite, Ba and V rich muscovite, quenselite, and kamaishilite (minerals identified by SEM-EDS and/or XRD, for details see Hîrtopanu, 2019).

X-ray powder pattern of Răzoare lindströmite: d spacing (Å) and Intensity ($I/I_o$): 3.64110(100); 3.5545(90); 3.16338(70); 3.14217(30); 2.56949(50); sample Rz531E. The X-ray data are very similar with those of Ontario lindströmite (Pring et al., 1998). In sample Rz528A lindströmite occurs associated with kieftite, in rhodochrosite, hydroxylapatite, eudydimite, quenselite, and hummerite veins.

Nickeline, NiAs, was determined in the sample Rz52B (sonolite, tephroite, apatite, clinohumite, danalite) as relics in the new Bi and Ni arsenate paganoite, $(Ni,Bi)AsO_5$. Paganoite was recently discovered (Roberts et al., 2001) as a new mineral, and was found on a single nickeline-veined quartz specimen from Johanngeorgenstadt, Saxony, Germany. The Răzoare paganoite occurs associated with nickeline, aerugite ($Ni_{17}As_6O_{32}$), bismite ($Bi_2O_3$), and native bismuth. The strongest lines of the X-ray powder diffraction pattern of Răzoare paganoite d spacing (Å) and Intensity ($I/I_o$): 3.0404(70); 3.43569(30); 3.22898(100); 3.06390(70); 3.05134(50); 2.61107(30); 2.11484(50); 2.09765(45); 2.79774(25). The data are very similar to those of Saxony paganoite.

The X-ray data were made on the complex ore samples. To obtain refined unit cell dimensions for these rare minerals and complete data, X-ray powder diffraction is needed for the monomineral samples. This study may be undertaken in the future.

## 5. SOME GENETIC CONSIDERATIONS OF Ni-Co-Sb-Mn-Fe ARSENIDES/ SULFARSENIDES

The source of mineralizing fluids and their exact nature and geneses are difficult to explain.

The old pyrrhotite of this assemblage has Ni and Co as trace elements (Ni = 180-400 ppm and Co = 190-300 ppm) (Udubaşa et al., 1996) which could be the source of the new appearance of the hydrothermal Ni, Co, Mn, Fe arsenides and sulfarsenides. This could have happened during the metamorphic recrystallization, as a result of the replacement of the pyrrhotite by pyrite, with the liberation of Ni and Co. The pentlandite could be a Ni source for later Ni arsenides. Also, the old magnetite of Mn-fayalite association contains some Ni (110ppm) and Co (130ppm) (Udubaşa et al., 1996), as trace elements.

The jacobsite of tephroite/manganese humites association has higher Ni and Co, as trace elements, than magnetite.

Some pyrrhotite samples show high As as a trace element (1000 ppm) (Udubaşa et al., 1996), which could be linked most probably to the presence of associated old maucherite ($Ni_{11}As_8$).

The source of arsenic could be an old arsenopyrite (?), which was destroyed by metamorphism because of its very narrow stability field. Also, the As source could be the initially premetamorphic sedimentary pyrite which might have contained small amounts of As. The enrichment in As is a common feature of many authigenic pyrites. The As accommodated in the first pyrite was liberated during metamorphic recrystallization as a result of the replacement of the pyrite by new metamorphic As-free pyrrhotite. Also, the Ni source of some arsenides could be the trevorite ($NiFe_2O_4$), and the Sb source of antimonides could be melanostibite $Mn_2(Fe, Sb)O_6$. The polyphase evolution (five stages) with sudden changes in physicochemical parameters of hydrothermal fluids proves its continuous feeding from a source that could be considered a small but intense hydrothermal activity in a very short time.

The old metamorphosed pyrrhotite - chalcopyrite - pentlandite - pyrite assemblage and most probably an old maucherite must be correlated with the new Ni-Co-

Mn-Fe arsenides and sulfarsenides of the two assemblages. The liberated Co, Ni, Sb, Bi, and As by metamorphism were remobilized by hydrothermal fluids as highly soluble chloride complexes and were precipitated inside cracks and cleavages of the grains. The changes in metamorphic hydrothermal solutions have been gradual and alternative, the same arsenides/sulfarsenides occur in two generations. The mineral assemblages and the comparison with similar As-dominated minerals in other deposits suggest that the complex arsenide/sulfarsenide minerals have formed at *T* around 300˚/400˚C, being genetically associated with local hydrothermal activity which accompanied a later lower grade metamorphism. On the other hand, the As-rich gersdorffite coexisting with rammelsbergite, according to experimental data, must have been formed at *T* above 500˚C (Spiridonov and Chvileva, 1995). The textural relations among Ni, Co, Mn, and Fe arsenides/sulfarsenides show frequent zonings, which reflect sudden changes in the composition of hydrothermal fluids. Also, their zonings depict a polyphase evolution. Later minerals overgrow and replace earlier ones. Usually, the center of the zoned grain is rich in Ni-Co-monoarsenide, Ni-monoarsenide (maucherite, nickeline), and Ni-Sb-monoantimonide (breithauptite). The diarsenides were deposited earlier than the Ni-Co triarsenides. The mineralization process trend is characterized by the As increasing, and the *T* decreasing of the hydrothermal fluids. The redox conditions that control the progressive oxidation of arsenic are highly variable, from the arsenide stage ($As^{-1}$) to sulfarsenide stage ($As^{3+}$). The Mn content more than that of Fe is a predominant feature of these new minerals of the Răzoare deposit. They are at least a manganoan variety, which could be a new mineral species if the Mn content is higher.

The mineralogical and genetic evolution of the Răzoare arsenides - antimonides - sulfarsenides - sulfantimonides - sulfides belongs to five stages:

A. Monoarsenides/monoantimonides of Ni, Co, Ni+Co, Sb: nickeline, breithauptite, modderite, maucherite manganoan, maucherite cobaltian;
B. Diarsenides of Ni, Ni-Co, Co, Mn, and Fe: rammelsbergite, rammelsbergite cobaltian, safflorite, löllingite;
C. Triarsenides/triantimonides. Triarsenides: Skutterudite, nickelskutterudite, linnaeite; Triantimonides: kieftite;
D. Sulfarsenides, sulfantimonides, and sulfbismuthides: sulfarsenides: cobaltite, gersdorffite, arsenopyrite, glaucodote, hutchinsonite; Sulfantimonides: willyamite, füloppite, benavidesite, clerite; Sulfbismuthide: lindstromite;
E. Sulfides: millerite, cattierite, bismuthinite, stibnite.

The first mineralized stage (A) is characterized by the occurrence of NiAs, CoAs, NiCoAs, NiSb, with low As content and high Ni, and Co, which evolved to higher As content in stage B and less Ni and Co, to highest As in stage C and less Ni and Co, to less As and higher S in stage D (the occurring of sulfarsenides, sulfantimonides, sulfbimuthides), and the final stage E was enriched in S, and no As, allowing the deposition of the latest sulfides of Ni, Co, Sb, and Bi.

In other metamorphosed manganese ores in Romania and the world, the origin and occurrence of the arsenides, sulfarsenides, and tellurides were well studied and there are similarities with Răzoare manganese deposit. In the Manganese Belt of Bistrita Mts. all lithology types of metamorphosed ore show concentrations of Ni, Co, Bi, As, Sb, Cu, Zn, U, Li, Th, etc., and REE trace elements, being similar to the trace element concentrations reported from sediments which are forming in hydrothermally active regions on the present sea floor (Hîrtopanu, 2023). The metamorphic evolution of the Mn ore of Manganese Belt (MnB) was achieved through repeated and superimposed metamorphic events, a fact explaining its complex mineralogy. The fluid phase composition ($CO_2$, $H_2O$, Cl, F, OH, As, and S) has a strong influence on the in-situ mineral transformations of MnB ore. Also, the repeated retrograde metamorphisms of manganese ore of MnB caused the spectacular mineralogical changes and the forming of zoned alkali pyroxenes and amphiboles, many Li-minerals, hydrated silicates with Cl and As (pyrosmalites, nelenite, sphalerite, etc.), many secondary Ni-Co-Bi-Ag-Sb sulfides, arsenides, selenides, etc. (Hîrtopanu, 2019; Hîrtopanu et al., 2024) formed after the completion /superimposed of the earlier Pb–Zn-Fe-Cu-Pb-Mn sulfides, and finally, many secondary arsenates grown on the arsenides and their varieties, by the changes in pH and oxidation state of fluids composition.

Haruna et al. (2002) showed that the oxygen isotope disequilibrium among all the analyzed minerals from the Nagasawa bedded manganese ores from Japan suggests that externally derived fluid phases were not important during their formation. A detailed petrographic, mineralogical, and genesis studies of ore samples of Nagasawa bedded manganese deposit made by Haruna et al. (2002), reveals that Fe-, Co-, Ni-, Cu-, Zn- As-, Te-, Pb-, and Bi-minerals (including native elements, sulfides, arsenides, and tellurides) are common and they were first concentrated in sea floor sediments (ferromanganese nodules) or sea floor hydrothermal fluids. These minerals of the Nagasawa deposit are closely associated with garnet in the pyroxmangite - garnet - amphibole ore (which was) metamorphosed from the rhodochrosite-chlorite -quartz unmetamorphosed assemblage. This assemblage has

commonly minor elements concentrated in chlorite and pyrite-bearing associations during diagenetic reconstitution of Mn oxides and hydroxides to manganese carbonates. Breakdown of the two associations by metamorphism into the garnet-bearing assemblage released the minor elements that subsequently reacted with $H_2S$, generated by the replacement reaction of pyrite by pyrrhotite to form minor sulfide and other minerals during metamorphism (Haruna et al., 2002).

The „accessory mineralization" of the sulfoantimonides, sulfoarsenides, sulfides, antimonides, arsenides, bismuthinides, tellurides, native Bi and Sb, etc., in manganese silicates rocks of the Triassic russian Sikhote-Alin chert formation mineralization was formed from the protolith material during metamorphism under the same conditions as the rock-forming minerals (Kazachenko and Perevoznikova, 2019).

## 6. THE SECONDARY ARSENATES GROWN ON Ni, Co, Sb, Mn, Fe ARSENIDES/ SULFARSENIDES

The appearance of large variety of manganese arsenates at the expense of arsenides/sulfarsenides/sulfides, alongside on the various secondary silicates, phosphates, sulfates, and carbonates, marks the transition to an oxidizing environment. The redox conditions that control the progressive oxidation of arsenic are highly variable, from the arsenide stage ($As^{-1}$) to sulfarsenide stage ($As^{3+}$), and to arsenate ($As^{5+}$) stage.

The arsenates, grown on arsenides/ sulfarsenides, present a wide occurrence and varieties containing Mn, Fe, Co, Sb, and Ni, as the main cations. They belong to the minerals of low-temperature affiliation. The textural relations in many optical images, show that the arsenates were formed at the expense of arsenides/sulfarsenides, substituting these minerals. The arsenoclasite, eveite, johnbaumite, grishunite, manganarsite, and many other secondary arsenates have been determined in the Răzoare ore (Hîrtopanu et. al., 2016). Manganostibite, a rare mineral with high As and Sb contents, was determined in the manganese humites association.

The manganostibite ($Mn_7SbAsO_{12}$) determined by X-ray analyses occurs as small black rounded grains in associated rhodochrosite to manganese humites. The paganoite, a Ni and Bi arsenate (Ni, Bi)$AsO_5$, the annabergite, $Ni_3(AsO_4)\cdot 8H_2O$, grown on Ni/arsenides/bismuthides, sulfarsenides, and the erythrite, $Co(AsO_4)_2\cdot 8H_2O$, grown on Co rich/arsenides/sulfarsenides, were also determined in the ore, in the two assemblages, rich in Mn and rich in Fe, as latest oxidized minerals (Hîrtopanu et al., 2016).

## 7. CONCLUSIONS

The Ni-, Co-, Mn-arsenides, antimonides, sulfarsenides, and sulfantimonides have been identified in the Răzoare ore for the first time in the rich Mn assemblage. The rich Fe arsenides, bismuthides, sulfarsenides, Bi-tellurides, and native Bi, hosted by the rich Fe assemblage, were also identified in the Răzoare ore for the first time. The native gold, as minute grains, occurs in both assemblages.

The old metamorphic primary pyrrhotite / chalcopyrite / pentlandite/ magnetite association, the first old mineralization stage, could be considered the source for the new/late mineralization of arsenides, antimonides, sulfarsenides, sulfantimonides, and tellurides. The arsenides of the new mineralization stage are characterized by decreasing the arsenic fugacity and strong increase in the sulfur fugacity, with the following succession of deposited/ precipitated minerals: (A) monoarsenides (maucherite, nickeline) as relics in (B) diarsenides (rammelsbergite, rammelsbergite-löllingite solid solutions series), (C) triarsenides stage (skutterudite, nickelskutterudite, and manganskutterudite), (D) sulfarsenides (gersdorffite, cobaltite, gersdorffite-cobaltite series), which marks the increase in the sulfur fugacity and decrease in arsenic content, and the five-stage (E) marks the high S enrichment, allowing finally the deposition of Ni, Co, Sb, and Bi sulfides. The Co-, Ni-, Mn-, Fe- triarsenides have grown over the Co-, Ni- diarsenides with which they form zonings and complex intergrowths, and the diarsenides growing over the monoarsenides.

The mineralogy of the Ni-Co-Mn-Fe arsenides/antimonides/sulfarsenides/sulfantimonides/Bi-tellurides/Bi-sulfotellurides/sulfides at Răzoare could turn out to be even more complex, and a modern study is needed. Their chemical compositions, which were here determined by SEM analyses, must be determined for accuracy by electron microprobe analyses in the future. Such a study is also necessary because these two large important assemblages, with their later small new mineralization of the arsenides/ antimonides/ sulfarsenides/ sulfantimonides/ Bi-tellurides/ sulfotellurides/ sulfides, and the latest arsenates formed at the expense of some of them, could be a large source of new and rare minerals.

**Acknowledgments**

The authors are very grateful to Prof. Peter W. Scott for his permanent assistance during the analytical/laboratory work at the Camborne School of Mines (CSM), Exeter University, Cornwall, UK in the period July-October 1996 during the collaborative work between the Geological Institute of Romania and Camborne School of Mines. Thanks are also given to physicist Antony Ball for the kind help

during the SEM and X-ray analyses performed in the CSM laboratories. Several X-ray analyses were performed at the Laboratory of Radiometry and X-ray, from the Geological Institute of Romania (Bucharest), for which the authors express their thanks. This study was partly supported by a scientific research grant allowed by the Ministry of Research, Innovation and Digitization (PN23-39-02-06/2023).

## REFERENCES

**Dobbe, R. T. M., Lustenhouwer, W. & Zakrzewski, M. A.,** 1994. *Kieftite, $CoSb_3$, a new member of the Skutterudite group from Tunaberg, Sweden.* Canadian Mineralogist, v. 32, no. 1, p. 179-183.

**Haruna M., Satoh H., Banno Y., Kono M. & Bunno M.,** 2002. *Mineralogical and oxygen isotopic constraints on the origin of the contact metamorphosed bedded manganese deposit at Nagasawa.* Canadian Mineralogist, Vol. 40, no. 4, pp. 1069-1089.

**Hîrtopanu P., Călin N. & Udubaşa S.S.,** 2024. *Nambulite and Natronambulite Occurrence in the Manganese Belt, Bistriţa Mountains, Eastern Carpathians, Romania.* Carpathian Journal of Earth and Environmental Sciences, vol. 19, no. 1, p. 89-102.

**Hîrtopanu P., Udubaşa G., Udrescu C., Cristea C. & Călinescu E.,** 1993. *Mineralogy of the Mn-Fe ore deposit Răzoare, Preluca Mts. I. Tephroite-manganese-bearing humites.* Rom. J. Mineralogy, 76, 1, p. 15-22.

**Hîrtopanu P. & Udubaşa G.,** 2015. *Minerals from Răzoare Mn-Fe deposit, Preluca Mountains, East Carpathians: new data.* Rom. J. Mineral Deposits, v. 88 (1-2), p. 11-28.

**Hîrtopanu P., Udubaşa G., Marincea Şt. & Dumitraş D.,** 2016. *Some secondary minerals grown on manganese humites association in Răzoare Mn-Fe deposit, Preluca Mts, East Carpathians, Romania.* 35th International Geological Congress, Cape Town, Abstracts Volume, paper nr. 2568.

**Hîrtopanu P.,** 2019. *New minerals and mineral variety for Romania*. 263 pp., Editura Vergiliu, Bucureşti.

**Hîrtopanu P.**, 2023. *Geochemistry and Origin of Banded Ore of Manganese Belt, Eastern Carpathians, Romania.* Rev. Roum. Géologie, Tomes 66-67, p. 19-37, 2022-2023, Bucharest.

**Kazachenko V.T. & Perevoznikova E.V.,** 2019. *Composition and Genesis of Accessory Mineralization in Manganese Silicate Rocks of the Triassic Sikhote-Alin Chert Formation.* Russian Geology and Geophysics, vol 60, no. 6, pp. 631-641.

**Murzin V.V., Bushmakin A.F., Sustavov S.G. & Shcherbachov D.K.,** 1996. *Clerite $MnSb_2S_4$ – a new mineral from Vorontsovskoye gold deposit in the Urals.* Zapiski Vserossijskogo Mineralogicheskogo Obshchestva, 125(3), p. 95-101.

**Nelen J.A. & White J.S.,** 1985. *Hutchinsonite from Quiruvilca, Peru.* The Mineralogical Record, 16 (6) 459-460.

**Oudin E., Picot P., Pillard F., Moëlo Y., Burke E.A.J. & Zakrzewski M.A.,** 1982. *La bénavidésite, $Pb_4(Mn,Fe)Sb_6S_{14}$, un nouveau minéral de la série de la jamesonite.* Bulletin de Minéralogie, 105, p. 166-169 (in French with English abstract).

**Pring A., Grguric B.A. & Criddle A.J.,** 1998. *Lindstromite from Cobalt, Ontario.* Canadian Mineralogist, 36, p. 1139–1148.

**Oberti R., Boiocchi M., Hawthorne F.C., Ciriotti M.E., Revheim O., & Bracco R.,** 2018. *Clino-suenoite, a newly approved magnesium-ironmanganese amphibole from Valmalenco, Sondrio, Italy.* Mineralogical Magazine, February 2018, Vol. 82(1), pp. 189–198.

**Solly R.H.,** 1905. *Some new minerals from the Binnenthal, Switzerland*. Mineralogical Magazine, 14, p. 72-82.

**Spiridonov E.M. & Chvileva T.N.,** 1995. *On the boundary between gersdorffite NiAsS and krutovite $NiAs_2$.* Dokl. Acad. Sci. USSR, Earth-Sci. Sect., no 341, p. 119-123.

**Spiridonov E.M. & Gritsenko Yu.D.,** 2007. *Ferroskutterudite, nichelskutterudite, and skutterudite from the Norilsk ore field.* New data on Minerals, M., 2007, vol. 42, p. 16-27.

**Roberts A.C., Burns P.C., Gault R.A., Criddle A.J., Feinglos, M.N. & Stirling J.A.R.** (2001) *Paganoite, $NiBi^{3+}As^{5+}O_5$, a new mineral from Johanngeorgenstadt, Saxony, Germany: description and crystal structure.* European Journal of Mineralogy, 13 (1), p. 167-175.

**Rouse R.C., Peacor D.R., Dunn P.J., Su S.-C., Chi P.H. & Yeates H.** (1994) *Samfowlerite, a new Ca Mn Zn beryllosilicate mineral from Franklin, New Jersey: its characterization and crystal structure.* Canadian Mineralogist, 32 (1), p. 43-53.

**Udubaşa G. & Hîrtopanu P.,** 1995. *Ore minerals in the Mn-Fe deposit at Răzoare, Preluca Mts.* Rom. J. Mineralogy 77, Suppl. Nr. 1, p. 46-47.

**Udubaşa G., Hîrtopanu P., İlinca Gh. & Valdman Şt.,** 1996. *The regionally metamorphosed Mn-Fe deposit at Răzoare, Preluca Mts, Romania*. Rom. J. Mineral Deposits, v.77, p. 3-20.

Received: 17.02.2025
Revised: 03. 08 2025
Accepted: 05. 08. 2025
Published:08. 08. 2025